ADVANCED MATERIALS INTERFACES
Open Access
www.advmatinterfaces.de

Dynamic Interfacial Architectures: Cruciferin-Stabilized Oil/Water Interfaces for Sustainable Emulsions

*Olaf Holderer, Jasper Landman, Joachim Kohlbrecher, Baohu Wu, Piotr Zolnierczuk, Maren Müller, Henrich Frielinghaus, Stephan Förster, Kuno Schwärzer, Leonard Sagis, Penghui Shen, Jack Yang, and Theresia Heiden-Hecht**

Stabilizing oil-water interfaces in emulsions by plant-based proteins provides sustainable and tunable ways for designing emulsions with specific properties, for food, healthcare, and pharmaceuticals. Cruciferin, a protein from rapeseed, has great potential as green emulsifier, but details about its structure and mobility at oil-water interfaces are largely unknown. Here, these properties are studied with small angle neutron and x-ray scattering, and neutron spin echo spectroscopy, analyzed by atomistic modelling of scattering curves and coarse-grained modelling, to gain insight into interface coverage, and molecular conformation and mobility at the interface. Cruciferin assumes trimeric conformations at the interface, as in solution, but with its protrusions from the central core of the subunits ("arms") more compressed. Interfacial mobility is only marginally lower than in solution, indicating the arms still transiently extend and preserve a network, for the first time revealing the mechanism how cruciferin forms highly elastic 2d gel-like oil-water interfaces, as observed in macroscopic rheology. The high interfacial mobility may help in self-repairing non-stabilized interfacial fractions, reducing coalescence. These findings provide a deeper molecular level understanding of proteins at oil-water interfaces, which can stimulate development of new plant-based emulsion products, and contribute to the global protein transition.

1. Introduction

Sustainable and green emulsions are increasingly important for producing plant-based materials, such as dairy alternatives, eco-friendly paints, and clean-label cosmetics.[1,2] One plant-based protein which has significant importance in stabilising emulsions is Cruciferin,[3] which can be extraxted from rapeseed. It is widely studied with respect to its molecular structure and classified as a globulin consisting of a larger α chain of about 32 kDa and a smaller β chain of 20 kDa, linked with disulphide bonds.[4,5] Cruciferin may exist as monomers (50 kDa), trimers (≈150 kDa) and hexamers (≈300 kDa) in solution.[6]

Cruciferin may be used in many different contexts: as emulsifier at oil/water interfaces,[7] or as a foam stabilizer at air/water interfaces,[8] and further for nanoparticle formation and encapsulation in many applications like food and pharmaceuticals.[9] A recent review of rapeseed proteins and their relevance for technical applications summarizes many aspects of the possible use cases.[10]

Some studies investigated the oil/water interface stabilized by Cruciferin in more detail.[7,11] When used as an emulsifier,[7,12] it forms emulsions with small oil droplets, which are surrounded by a stiff viscoelastic interfacial layer with a low interfacial tension.[7] Several characterization techniques indicated that depending on the ionic strength of the buffer,

O. Holderer, B. Wu, M. Müller, H. Frielinghaus, T. Heiden-Hecht
Forschungszentrum Jülich GmbH
Jülich Centre for Neutron Science
Lichtenbergstrasse 1, 85747 Garching, Germany
E-mail: t.heiden-hecht@fz-juelich.de

J. Landman, L. Sagis, P. Shen, J. Yang
Wageningen University and Research
Bornse Weilanden 9, Wageningen 6708WG, Netherlands

The ORCID identification number(s) for the author(s) of this article can be found under https://doi.org/10.1002/admi.202500368

DOI: 10.1002/admi.202500368

J. Kohlbrecher
Paul-Scherrer-Institut
Forschungsstrasse 111, Villingen 5232, Switzerland

P. Zolnierczuk
Neutron Scattering Division
Oak Ridge National Laboratory
P.O. Box 2008, Oak Ridge TN 37831, USA

S. Förster, K. Schwärzer
Jülich Centre for Neutron Science
Forschungszentrum Jülich GmbH
52425 Jülich, Germany

dissolved Cruciferin may be present mainly in hexameric or trimeric structures.[13] While the molecular state of cruciferin in solution has been extensively studied, many research questions about the detailed interfacial structure of Cruciferin at the oil/water interface, including its interface coverage and its in-plane association (i.e., how it forms 2D viscoelastic gel-like structures at the interface), remain open. Information at this structure level is very important for the development of plant-protein based systems, and could help to understand detrimental effects of certain extraction methods on functionality of proteins, or simply the significant batch-to-batch variations often observed in the scientific literature, a huge problem many other plant-based proteins also suffer from. Developing strategies to resolve this structure level is therefore highly relevant on a much broader scale, and could give a significant impuls to the development of plant-based products, thereby promoting the global protein transition.

Scattering techniques, such as Small Angle Neutron or X-ray Scattering (SANS/SAXS), have proven their capability to provide insight into structural properties on mesoscopic length scales, like the overall shape of proteins.[14] Even proteins adsorbed at oil/water interfaces have been studied.[15] SANS provides the unique ability to vary the contrast to highlight different parts of a complex multicomponent mixture.[16] The molecular structure of protein-stabilized emulsions can be accessed with SANS.[17] In a previous study, we investigated the interfacial structure for β-lactoglobulin with a molecular weight of 18 kDa at the oil/water interface at pH 7.[15] We calculated the interface coverage and, thus, the critical interfacial tension of the protein in the emulsion and characterised the association of this protein at the oil/water interface.[15]

The structure of proteins in solution and at the interface of emulsions, plays an important role in the protein's and interfacial dynamics, and hence in emulsion stability. On macroscopic length scales, the mechanical properties of interfacial protein films at the oil/water interface can be characterized using surface rheology, using for instance drop tensiometry, as shown for dairy and rapeseed proteins in ref. [18,19].[7,8] On molecular length scales, neutron spin echo (NSE) spectroscopy is suitable for observing mobility on molecular length scales and nanosecond time scales relevant for diffusion of proteins[20] and interfacial undulations of oil/water interfaces.[21]

Details about the molecular structure in solution, its conformation at the interface, its overall interfacial structure, and the mobility of Cruciferin at the oil/water interface are still largely unknown. The current article aims to elucidate the details of interfacial stability of oil/water interfaces stabilized with Cruciferin on a molecular level. SANS and SAXS can provide structural insight, while NSE is used for the first time on emulsion systems to provide a new view into the molecular mobility of the interface components on the nanoscale.

Cruciferin will be present in a hexameric or trimeric form in solution, according to the newest literature findings. There is a long-standing debate on whether proteins show a significant degree of unfolding after adsorption at an interface, and take on a totally different conformation to the one in solution. In view of the large size and the compact structure of cruciferin we would actually expect that the molecular structure changes barely upon adsorption at the oil/water interface. Here, we aim to identify the actual molecular structure of cruceferin at the interface, by comparing the experimental SANS curve of a Cruciferin-stabilized emulsion, with focus on the interface (by contrast variation), to a calculated curve presenting the structure of a trimer and hexamer in solution, obtained from a protein data bank. We also measure the interfacial mobility for Cruciferin at the oil/water interface via NSE for the first time, and show that the Cruciferin molecule has a lower mobility at the interface in comparison to its mobility in solution. The investigation of the molecular structure in solution and at the oil/water interface via SANS and SAXS, the interfacial dynamics via NSE, is extended further with a characterization of the structure of the emulsion itself via static light scattering. We aim to show how this combination of scattering techniques (SANS, SAXS and NSE) is an innovative toolset to characterise interfacial structure and mobility of proteins in general.

2. Experimental Section

2.1. Preparation of Protein Solutions

Proteins were isolated according to ref. [7]. The Cruciferin extract had a protein purity of 80.2 %, and a protein solubility at pH 7.0 of 82.1 %. The remaining 19.8% of non-protein material was expected to be mostly carbohydrates. The cruciferin extraction method was a mild-extraction, which preserves the protein nativity, but may co-extract small soluble carbohydrates, which were non-surface-active. Details about the molecular size distribution or interfacial properties of the Cruciferin extract were summarized here.[7] Protein solutions were made by dissolving a specific amount of Cruciferin-isolate in ultrapure water (ariumpro, Sartorius AG, Göttingen, Germany). After stirring for three hours at room temperature solutions were filtered using a Millex-GP PES-membrane filter (0.22 µm, Merck, Cork, Ireland) to remove any large aggregates.

2.2. Preparation of Emulsions

Medium-chain-triglyceride oil (MCT-oil) was kindly provided bei IOI OLEO (Witten, Germany) and is composed of 60% caprylic and 40% capric triglyceride. MCT-oil was purified with Florisil(Carl Roth GmbH, Karlsruhe, Germany) in order to eliminate surface active contaminents prior to use. An amount of 5 wt.% MCT-oil was added to the filtered protein solutions and emulsified using an Ultra Turrax T18 digital (IKA-Werke, Staufen, Germany) at 25 000 rpm for 4 min.

2.3. Oil Droplet Size Distribution

The oil droplet size was measured with static light scattering (LA960V2, Horiba, Kyōto, Japan). Emulsions were diluted in distilled water. The refractive indices were set to 1.450 and 1.333 for the dispersed and continuous phase, respectively. The measured 10% percentile, median, and 90% percentile are number based values.

2.4. Small Angle Neutron Scattering (SANS)

In small-angle neutron scattering, the sample was illuminated with a collimated neutron beam. The scattered intensity behind

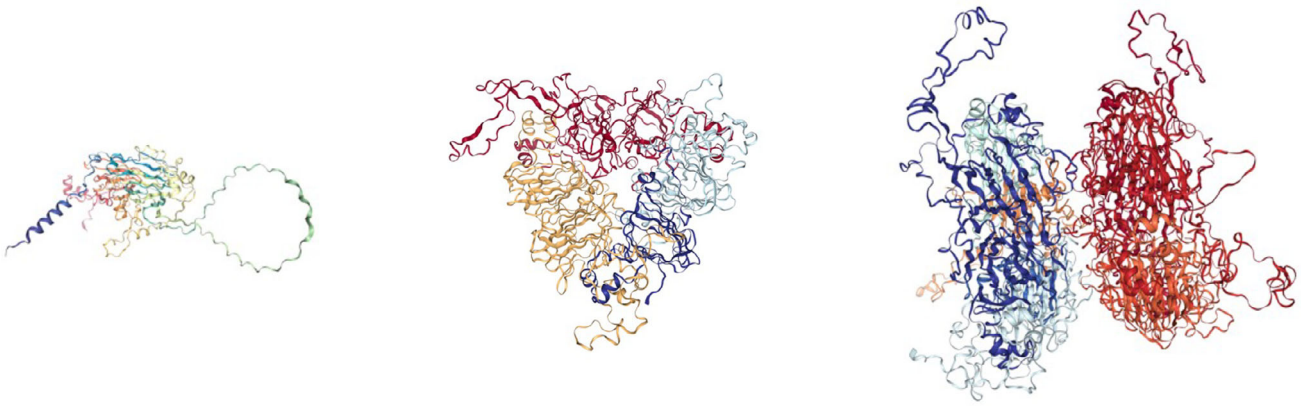

Figure 1. Monomer, trimer and hexamer of cruciferin, which all are present in solution. Data derived from the rcsb protein data bank[22] and AlphaFold.[23]

the sample was recorded and analyzed. For an isotropic sample with no preferential orientation, the radially symmetric scattering pattern was typically radially averaged. The scattering angle Φ was converted into a reciprocal scattering vector Q (or its modulus due to radial averaging) with $Q = 4\pi/\lambda \sin(\Phi/2)$ at the neutron wavelength λ. The scattering cross-section $d\Sigma/d\Omega(Q)$ as a function of Q was then an ensemble average of the particles in the sample (i.e., a product of the form factor of the particle shape and the structure factor of its spatial arrangement, if concentrated enough). The scattered intensity dependant on the scattering length density difference between the different components, for a protein in water between protein and water (or heavy water, D_2O). Especially the possibility of varying the contrast by using different isotopes (H_2O vs D_2O) and the sensitivity to light elements makes neutron scattering a very powerful technique. Details of scattering theory can be found in ref. [24].

Small angle neutron scattering experiments were carried out at the SANS-1 beamline at PSI, Villigen, Switzerland.[25] Raw data correction to obtain radially averaged scattering intensities with absolute scale were done with the BerSANS software.[26] The experimental setup was comparable to a previous publication.[15]

2.5. Small Angle X-Ray Scattering (SAXS)

Similar to neutron scattering, also SAXS measures the scattering cross-section $d\Sigma/d\Omega(Q)$ as a function of Q on the same length scales as SANS, but with different contrast conditions. X-rays were principally more sensitive to variations in atomic mass and changes in the light elements typically present in soft matter were more challenging. But modern X-ray instruments (lab based or synchrotron sources) allow to obtain valuable results also for proteins, and the different contrast conditions provide complementarity to SANS. Small angle x-ray scattering experiments had been carried out at the in-house SAXS beamline KWS-X at JCNS (XENOCS XEUSS 3.0 XL Garching Version), MLZ Garching, Germany, equipped with a Ga-Kα liquid metal jet source (wavelength $\lambda = 1.314$ Å).

The experimental setup was comparable to a previous publication.[15]

2.6. Neutron Spin Echo Spectroscopy (NSE)

Neutron spin echo spectroscopy provided access to diffusive motion and thermal fluctuations of macromolecules. It offered the

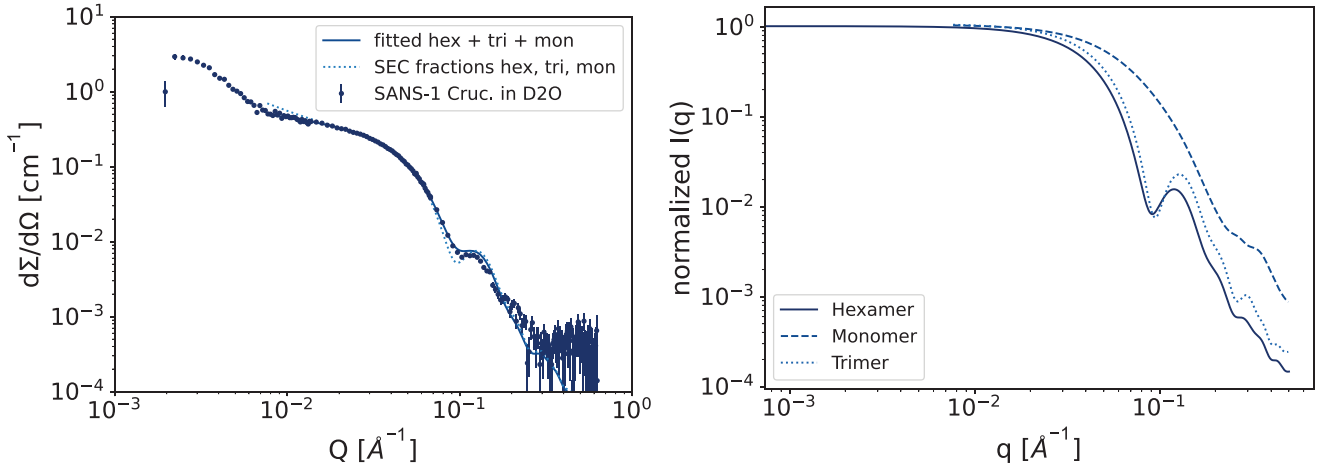

Figure 2. Left: Solution scattering, fitted with the calculated SANS curves of the possible structures (monomer, trimer, hexamer). Right: Normalized calculated SANS intensities from CRYSON.

high resolution required for probing the diffusion of proteins in solution, i.e., on length scales of $2\pi/Q$ of some nanometers the time correlation function was measured on time scales of some ten nanoseconds in the present case. This was achieved by encoding and decoding the velocity change of the neutron in a not purely elastic scattering process ("Quasi-Elastic Neutron Scattering", QENS) by a number of spin precessions of the polarized neutron beam in a magnetic field before and after the scattering process. A detailed introduction can be found in refs. [27,28].

NSE experiments were carried out at the SNS-NSE (BL15) at Oak Ridge National Laboratory, Oak Ridge, TN.[29] It provides excellently shielded environment against radiation and perturbing magnetic fields and was therefore perfectly suited for experiments with low concentration, requiring stable experimental conditions. Nonetheless it had to be pointed out that the protein concentrations studied here remain a challenge for NSE experiments. The incoherent scattering of the solvent (D_2O) already contributes considerably to the depolarization of the polarized neutron beam and restricts the accessible Q-range to only lower Q-values. Care had been taken that the average scattered intensity was constant over the time of the experiment to guarantee that the emulsion stability was good enough for the experimental duration.

Protein solution, emulsion and background solution (D_2O) were measured under the same conditions in quartz cuvettes with 4 mm path length. Grafoil stacks were measured as resolution. Data reduction was performed with the NSE data reduction software DrSPINE available at the instrument.[30]

3. Results and Discussion

3.1. Molecular Structure of Cruciferin in Solution

Cruciferin may be present in solution in its monomeric, trimeric or hexameric form. **Figure 1** shows structural representations of Cruciferin. The protein structures are obtained for the monomer from Alphafold[23,31] (structure AF-P33525-F1), and for the trimer and hexamer from the protein databank (structure 3KGL[22,32]). All three forms show the existance of protrusions from the central core of each monomeric subunit, which will play a role in the discussion of the Cruciferin binding to the hydrophobic interface in the emulsion in Section 3.3, where these protruding subunits are named "arms". An assessment of the mixture in solution can be obtained by fitting the SANS intensity with the weighted form factors of the three forms of Cruciferin. The SANS form factor has been calculated with CRYSON in the online ATSAS software suite[33,34] from the pdb files. The normalized SANS form factors are fitted to the experimental data with 0.25 wt.% cruciferin in D_2O. **Figure 2** shows the experimental data together with the fitted curve, **Table 1** summarizes estimates of the relative volume fractions from the SANS intensities, deduced from the expected forward scattering intensities $I_0 = \Phi(\Delta\rho)^2 V_{\text{protein}}$ for the three subtypes. The increasing intensity at low Q is taken into account with a global Ornstein-Zernike like structure factor[35] contribution for possibly larger aggregates.

The distinction between hexamer and trimer is not very precise from the fit with the calculated curves, but the forward scattering intensity I_0 expected for a solution of Cruciferin hexamer only would be 1.1 cm^{-1} (at a concentration of 0.25 wt.% and a contrast $\Delta\rho \simeq 3.5 \times 10^{10}$ cm^{-2}), significantly more than the plateau around and below 0.01 $Å^{-1}$ in Figure 2. We can therefore assume that the main fraction in solution is the trimer, as also deduced from SEC experiments (see Table 1).

Table 1. Forward scattering intensities and deduced volume fractions compared volume fractions obtained from size exculsion chromatography (SEC).[8] Relative errors of the SANS volume fractions are estimated to be of the order of 10%.

Type	$I(0)_{calc}$ [cm^{-1}]	I_n/I	$I(0)_{fromFit}$ [cm^{-1}]	Vol fraction	SEC
Hexamer	1.10	0.00	0.01	0.01	13
Trimer	0.55	0.81	0.45	0.81	80
Monomer	0.18	0.19	0.10	0.18	7

3.2. Structure of Emulsions: Oil Droplet Size

The emulsions were characterized with respect to oil droplet size distribution for all protein concentrations from 0.1%–0.5%, measured via static light scattering. It was observed that all concentrations exhibit small oil droplets with a narrow size distribution. The number-based 10%-percentile (D10), median (D50) and 90%-percentile (D90) are displayed (**Figure 3**). The values varied from 1.82 to 2.08 µm, 2.99 to 3.52 µm and 5.91 to 6.85 µm for the D10, D50, and D90, respectively. Here, the smallest value always refers to the lowest protein concentration, except for the D50-value of the emulsions at 0.5% protein, which decreased slightly compared to the 0.25% protein emulsion. However, the observed differences are not significant.

With an increasing protein concentration, more interfacial area can be stabilized, resulting in a finer dispersed system. Yang and colleagues reported a more evident decrease in the individual droplet size ($d_{3,2}$) from 2.5 to 0.7 µm as the protein concentration increased from 0.2% to 1.0% during studying the emulsification properties of Cruciferin proteins.[7] A further decrease in the droplet size with increasing protein concentration was not that pronounced any more. However, a direct comparison of the droplet size to our findings is not possible as in those studies the 10 wt.% rapeseed oil emulsions were prepared using a high-pressure homogenizer after pre-emulsification with an Ultra Turrax.[7,36]

The cruciferin emulsions are highly stable in long-term time ranges, up to 57 days without flocculation or coalescence, as shown by Yang et al.[7] **Figure 4** gives an impression of the stability of the emulsions at the three Cruciferin concentrations (0.1%, 0.25%, and 0.5%) right after preparation and after 1 day and 2 days (which has been confirmed also by repeated SANS measurements with a dwell time of about 6h without a change in scattering intensity, indicating that the emulsion stayed intact during the experiment).

3.3. Interface Structure

Emulsions stabilized with Cruciferin were characterized with SANS and SAXS. The strength of neutron scattering was exploited by using deuterated MCT oil[37] and D_2O for an

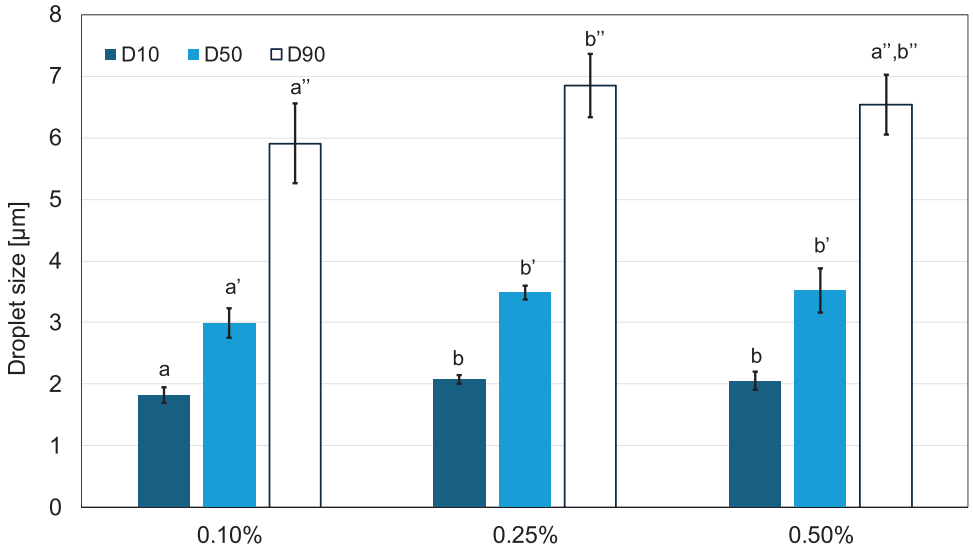

Figure 3. Oil droplet size distribution of emulsions prepared with different protein concentration. Emulsions contain 5 wt.% MCT-oil and 0.1 wt.%-0.5 wt.% cruciferin protein, respectively. Oil droplet size in µm is evaluated in 10%-percentile, median and 90%-percentile. Error bars display the standard deviation and different letters indicate significant difference, $p < 0.05$, within the percentile group.

interface-sensitive contrast. Together with the full oil droplet contrast (protonated MCT, D_2O) this allows the determination of the interface coverage of the oil droplets, as explained in Ref. [15]. In "interface contrast" with D_2O and dMCT, the interfacial layer has a different neutron scattering length density than the solvents on each side, which results in the typical Q^{-2} power law decay of the SANS intensity at small Q (**Figure 5** (left), open circles). On the other hand, the full "droplet contrast" with protonated MCT and proteins versus D_2O results in a Porod regime with a Q^{-4} power law decay (Figure 5 (left), continuous line). From the ratio of the SANS intensities $I_{\text{interface}}/I_{\text{Porod}} \times Q^2$ of two power law decays at low Q, the surface coverage can be calculated according to the formallism described in Ref. [15], (assuming a protein layer thickness of 69 Å[8]).

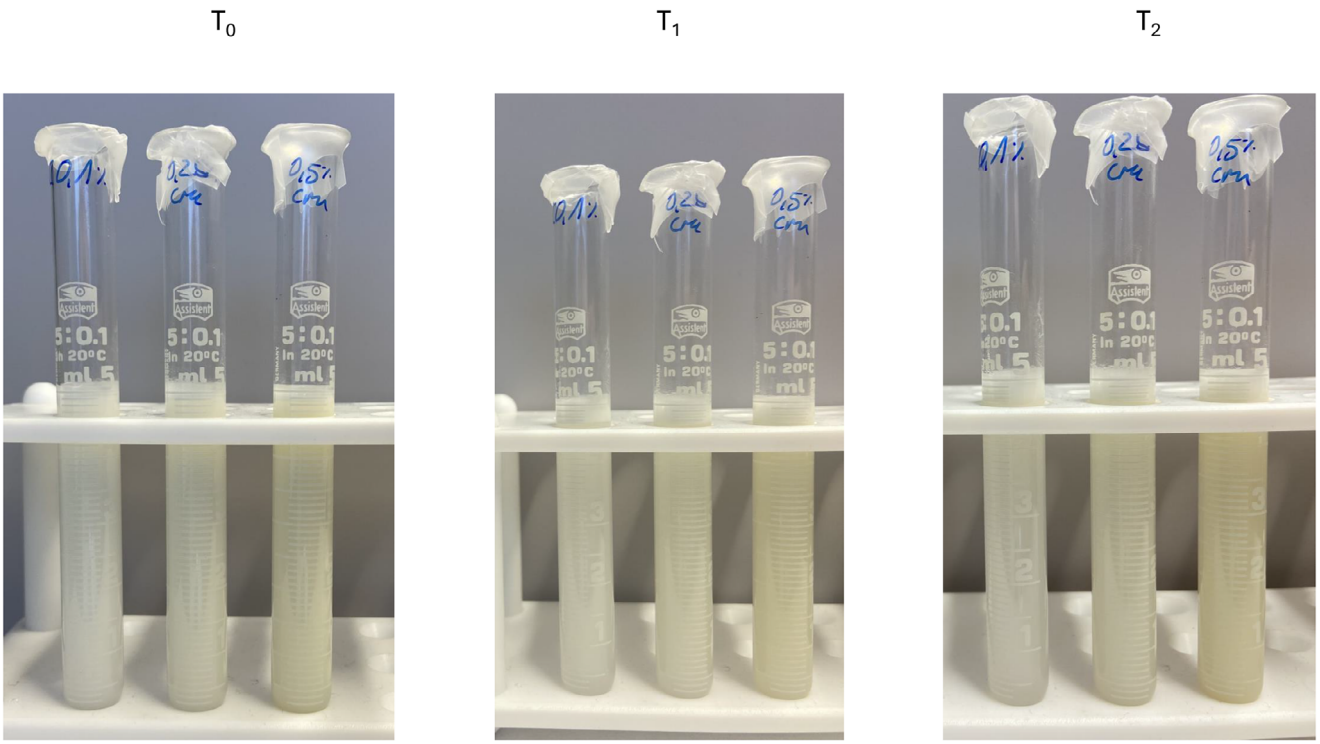

Figure 4. Photographs of the emulsion with 0.1%, 0.25%, and 0.5% Cruciferin (from left to right in each photo) right after preparation (T_0), after 24h (T_1) and after 48h (T_2), showing that the emulsions are stable for the duration of the SANS and NSE experiments.

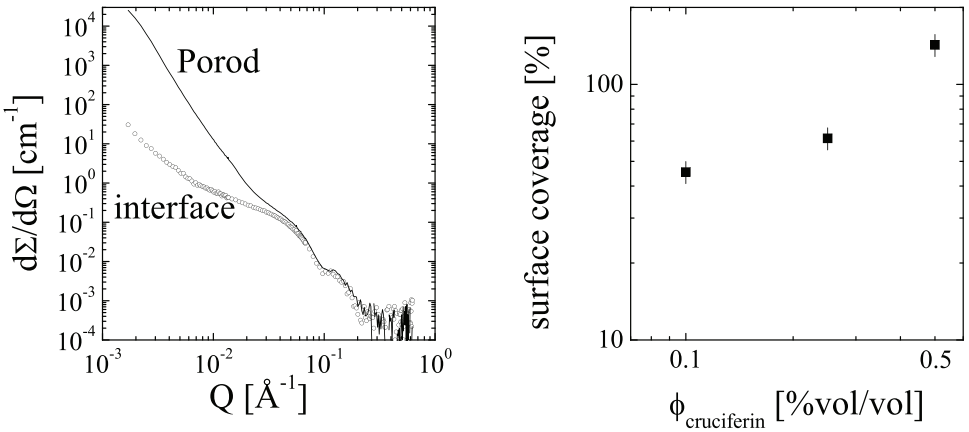

Figure 5. Emulsion stabilized with Cruciferin in two contrasts (left for 0.25 wt.% Cruciferin) and the resulting interfacial coverage as a function of Cruciferin concentration.

Figure 5 shows the two contrasts for an emulsion with 0.25% Cruciferin and 5% MCT oil, and the calculated interface coverage of the oil droplets as a function of Cruciferin concentration. A concentration of 0.25% corresponds to an almost full coverage of the oil droplets, and at 0.5% , the interface coverage of >100% indicates that there is more material than required for a monolayer interface coverage, and most likely, a multilayer is formed.

The scattering intensity of SAXS data revealed that the protein structure which dominates at $0.02 \approx Q \approx 0.2$ Å^{-1} does not change in the emulsion, hence the integrity or fractions of monomers, trimers and hexamers of the Cruciferin seem to stay as those in solution. At high $Q \approx 0.37$ Å^{-1}, a correlation peak is visible in the emulsion, which is missing in the solution, and this discrepancy might be attributed to a partial ordering of some layers of molecules of the MCT oil at the interface to the water phase in the vicinity of the proteins. Ordering of triglycerides at air-water interfaces has been observed e.g. in Ref [38]. Some preferential ordering into domains resulting in a broad peak in MCT has been reported in the Q-range of 0.2–0.4 Å $^{-1}$ e.g., in Refs [39, 40]. At low Q, the µm-sized oil droplets of the emulsion are visible. In the SAXS contrast, where the electron density variation matters, the main contribution comes from the proteins themselves, and not from the contrast between oil and water (similar to D_2O/dMCT contrast in SANS).

For the stable 0.1% emulsion (where clearly oil droplets exist, as measured with SLS), the droplet scattering is not pronounced (**Figure 6**, left). The higher concentrations show an increase in intensity, which roughly follows a power law with an exponent of −2 (if the difference between the remaining increase of the protein solution and the emulsion is taken). The intensity of the power law part increases by a factor of 1.16 between the 0.25% and 0.5% emulsion (with $I(Q = 0.005) - I(Q = 0.05)$ of the emulsion, minus the same for the solution, taken as the interface layer factor), which indicates that the volume occupied by the interface layer increases only moderately with concentration and above a protein concentration of 0.25% part of the Cruciferin is most probably in solution and not at the interface. For the lowest concentration, the interface coverage seems to be too low to result in interface scattering, hence there only the individual proteins are visible.

From the measured SANS and SAXS curves, we reconstructed the real space pair distribution function $P(r)$, and a representative real space bead model using the softwares DENFERT for the inverse Fourier transform,[41] and DAMMIF from the ATSAS package for the real space structure.[42] The latter allowed us to assume a threefold P3 symmetry for the structure that accounts for the dominating trimer structure of the protein. For all calculations, we considered only the Q-range between $Q \approx 0.01$ Å^{-1}

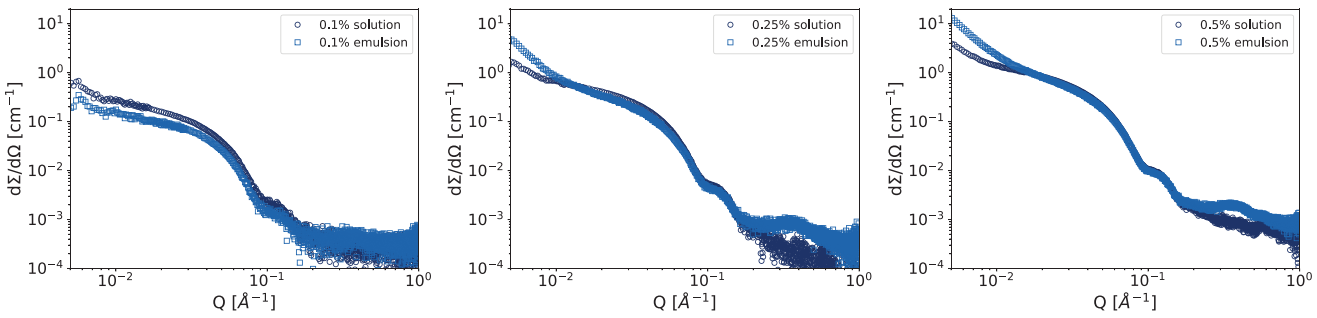

Figure 6. Cruciferin in solution and emulsions with three different protein concentrations (0.1%, 0.25%, and 0.5% from left to right). At low Q, the excess scattering of the oil droplets is visible, at high $Q \approx 0.37$ Å^{-1}, a correlation peak arises in the emulsion which might be due to some partial ordering of the MCT oil at the interface layer.

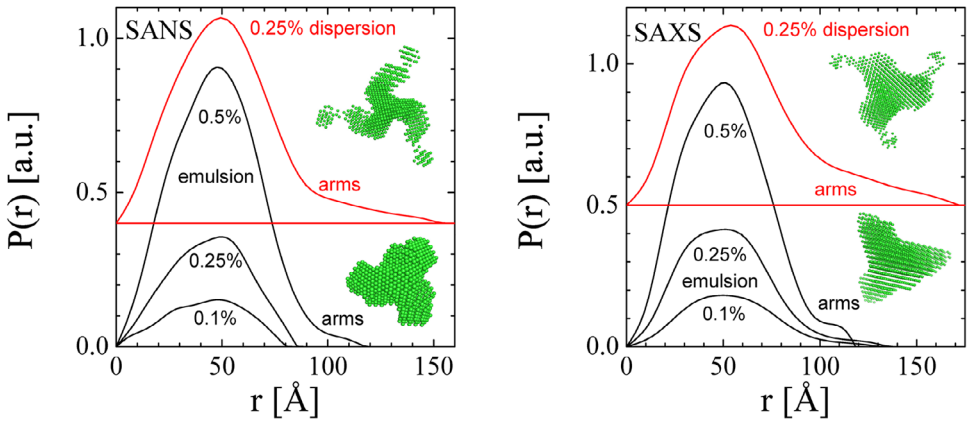

Figure 7. The real space pair correlation function $P(r)$ that is obtained from SANS and SAXS. It describes the protein structure in real space. For the emulsion, $P(r)$ for three different protein concentrations is displayed (0.1%, 0.25% and 0.5%), while for the aqueous solution only the 0.25% case is shown. One clearly sees that the long side arms of the protein are stretched wider in the aqueous solution. The real space reconstructions are also displayed in green where a P3 symmetry was assumed.

(below which the droplet structure dominates) and the MCT-oil correlation peak ($Q \approx 0.17$ Å^{-1}). Apart from that, we fitted an Ornstein-Zernicke-like structure factor[35] to the residual low-Q end of the data in order to divide by it. The obtained correlation functions $P(r)$ are displayed in **Figure 7**. One clearly sees a mass distribution of the globular protein part between 0 and 90 Å. This part is nearly unchanged between the aqueous solution and the emulsion case. However, lengthy "arms" are also visible at distances of $r = 90$ to 160 Å. They fully stretch in the solution case, and stay closer to the globular part in the emulsion. For the protein concentration of 0.25%, the real space reconstructions are also displayed (in green). Here, one clearly sees the structure of the side arms in the solution, which vanishes almost completely in the case of the emulsion. The cruciferin is present in trimers, hexamers and monomers, with the trimeric fraction being dominant. Table 1 summarizes the results from SANS and SEC measurements. The real space bead model described above explicitly assumes a three-fold symmetry, which ignores the minority components. But since we compare directly the solution structure with the emulsion structure, we think that remaining contributions of the smaller fractions of monomers and hexamers do not make this analysis invalid, since their possible contribution is present in both cases. We mainly observe a change in configuration of the real space reconstruction between solution and emulsion, with the more compact configuration at the emulsion interface. From the current experiments, we can not further quantify the possible influence of the minority components, this would require additional experiments with the different components. The same holds also concerning the possible contribution from the remaining small carbohydrate fractions, which could not be removed in the mild protein purification steps, as described in the Experimental Section 2.1. The direct comparison between solution and emulsion is in our point of view not touched by this fraction, the small carbohydrates only would contribute marginally, since the scattering contribution depends quadratically on the molecules volume.

The compression of the arms is likely due to the relatively high surface coverage (Figure 5). This also means that the protein is capable of forming networks that make the whole interface rather elastic, as seen by surface dilatational rheology experiments.[7]

3.4. Solution and Interfacial Mobility

Neutron spin echo spectroscopy (NSE) provides insight into thermally driven motion on molecular length- and time-scales. **Figure 8** shows the normalized intermediate scattering function $I(Q, t) = S(Q, t)/S(Q, t = 0)$ at $Q = 0.056$ Å^{-1}, i.e. on length scales of about 10 nm.

Simple Stokes-Einstein diffusion results in a decay according to $I(Q, t) = e^{-(DQ^2t)}$, with a diffusion constant given by $D = k_BT/(6\pi\eta R)$, where R is the particle radius, in a medium with a viscosity η, at temperature T. Experiments of Cruciferin in solution were carried out in D_2O, the emulsion experiment was done in interface contrast with D_2O and deuterated MCT oil, at a Cruciferin concentration of 0.25%, where the oil droplets are almost

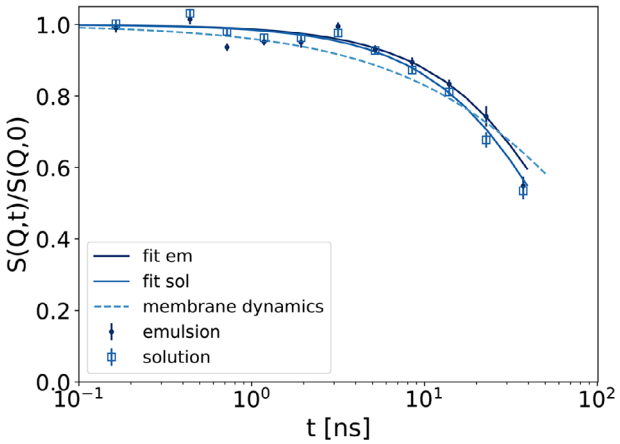

Figure 8. Intermediate scattering function measured with NSE of the protein solution and the emulsion at a scattering vector of Q = 0.056 Å $^{-1}$. The dashed line shows the expected curve shape for a pure membrane fluctuation with a stretched exponential behavior.

fully covered according to the SANS experiments, with practically no free protein in solution.

Membrane fluctuations probed with NSE occur, for example, in lipid vesicles, where thickness fluctuations of lipid bilayers[43] or influences of cholesterol on lipid membranes[44] can be investigated. The bending rigidity κ is deduced from the intermediate scattering function from a theory developed by Zilman and Granek,[45] where the membrane height correlation function is related to its elasticity. The intermediate scattering function is in this case $I(Q,t) = e^{-(\Gamma t)^{\beta}}$, with the relaxation rate $\Gamma \propto Q^3/\sqrt{\kappa}$ and the stretching exponent $\beta = 2/3$. The Q dependence (or inverse length scale dependence) allows therefore to distinguish between a diffusive Q^2 and a membrane behavior with Q^3,[43,45] a sufficient time window allows additionally to observe the curve shape described by the strechting exponent β. More subtle effects can be addressed,[46] especially concerning variations of the membrane elasticity and membrane viscosity effects. Here, we mainly want to compare the relaxation rate of the oil droplet interface of an emulsion with that of the Cruciferin proteins in solution with limitations related to the reduced Q-range available in the experiment.

A gel-like structure as deduced from dilatational rheology,[7] possibly formed by the arms of the protein at the surface, can lead to fluctuations, which exhibit a curve shape of $I(Q,t)$ similar to a simple exponential decay and with a Q^2 dependence, as in Stokes-Einstein diffusion,[47] in contrast to Q^3-dependent interface fluctuations. Here, only a single scattering vector Q could be measured, which only allows for distinguishing different decay mechanisms via the curve shape (single exponential or stretched exponential). Therefore, in both cases, i.e., protein in solution and at the interface of oil droplets in the emulsion, the first step of analysis was to determine the corresponding diffusion constant.

The diffusion constants D obtained from the fits in Figure 8 are 4.7 ± 0.4 $Å^2ns^{-1}$ (or 10^{-11} m^2s^{-1}) for the Cruciferin in D_2O and 4.1 ± 0.5 $Å^2ns^{-1}$ for the emulsion stabilized with the same amount of Cruciferin. The diffusion of the whole oil droplets is much slower and outside of the time window of NSE. The decay of $I(Q,t)$ comes from the mobility of the proteins in both cases. The only slight reduction in the diffusion constant indicates that the proteins at the oil droplet interface still have remarkable mobility on length scales of the experiment (i.e., about 10 nm). If the protein motion is separated into a 2D component at the surface of the oil droplet (2/3 of the bulk diffusion constant for 2 instead of 3 dimensions) and a 1Dcomponent perpendicular to the interface (1/3 of the bulk diffusion), the 2D surface mobility is apparently only very slightly reduced compared to the "free" 2D mobility. Also, the remaining perpendicular component only appears to be slightly reduced since the overall reduction D is only about 13 %. We postulate, therefore, that the proteins at the interface are still quite mobile and perpendicular to the interface. As a comparison, the expected curve shape of 2D interface fluctuations according to the Zilman-Granek model is shown, which would result in a stretched exponential decay with a stretching exponent of 2/3, which does not reflect well the curve shape measured here. The z-contribution might, therefore, behave also more like a diffusive contribution in a harmonic potential, which pulls the fluctuating proteins back to the interface as a restoring force. Principally it is possible to resolve the length-scale dependence of the relaxation rate, if a larger Q-range is covered experimentally. Plotting Γ/Q^2 versus Q shows a constant value for diffusive behavior or a linear increase for the typical membrane undulation behavior, which is proportional to Q^3. Additionally the curve shape with the streching exponent β can show possible deviations from a simple exponential decay, if the covered time range is large enough (and larger than in the current experiment that the intermediate scattering function decays close to zero), which would allow to separate different mechanisms of diffusion. Both, a larger Fourier time range and Q-range was for the current experiment out of reach, but as a first experiment on such a very dilute (for typical NSE conditions) emulsion system already the high mobility in emulsion is from our perspective very remarkably. For a general discussion on dynamics accessed by NSE we refer to the literature[27]

The high mobility of the protein-covered interface must be due to the type of network formed by the protein. If it is formed by the compressed arms as seen in the protein structure data, there must still be quite high flexibility in the arms that allows for transient extensions to a high degree, while keeping the network intact. Such a mechanism can potentially explain the high stability of cruciferin-stabilized emulsions, since it allows for a high degree of stretchability of the interface. This stretchability was also evident from dilatational rheology measurements using large amplitude oscillatory dilatation, where the dilatational storage modulus decreased only to a small extent in a strain range up to 20% deformation (from 30 to 23 mN/m).[7] The NSE experiments are sensitive to the scattering signal from the cruciferin form factor, which clearly dominates the relevant Q-range. The protein mobility comes therefore truely from cruciferin. The influence of the possible fraction of carbohydrates on the protein network at the surface is not accessible in the current experiment.

4. Conclusion

Scattering techniques from SANS, SAXS to NSE proved their applicability to investigate oil/water interfaces within emulsion systems in detail. These scattering techniques may be applied to any other protein or even interfacial active substance. Within this publication, we focused on the interfacial structure and mobility of Cruciferin as one sustainable protein.

For the interfacial structure, modelling of the scattering curves with atomistic structures as well as coarse grained modelling showed that mainly trimers are present in solution, and at the interface. In solution, cruciferin seems to take on a more extended structure with its side arms stretched out from the center, whereby the arms characterize just an elongated part of the tertiary of the protein. At the oil/water interface of the droplet, the structure is more compressed, and the arms are less extended.

Using SANS measurements in different contrasts (interface contrast or full droplet contrast) also by using deuterated MCT oil, allowed us to obtain the interface coverage in the emulsions, showing that for a 5% oil/water emulsion, a densely covered interface is obtained with Cruciferin concentrations between 0.25 – 0.5 wt.%. In comparison, for β-lactoglobulin, the interface was also fully covered with protein at a concentration of 0.25 wt.% protein. However, additional β-lactoglobulin associated as dimers was present in the water phase.[15] For Cruciferin, the additional

proteins above a fully covered interface appear to form a multilayer structure at the interface of the oil droplets.

For the interfacial mobility, the first NSE experiments on emulsion systems revealed that the proteins still possess a rather high mobility at the interface, and its dynamics resembles more the dynamics of density fluctuations in gels[47] than a pure membrane undulation of a thin membrane sheet.[43,44] From this result, it seems reasonable that also in the plane of the interface, the Cruciferin can move on length scales of some nm (the length scale of the NSE experiment. At longer length scales, the arms of the Cruciferin trimers might form an elastic network. Observing this with NSE on molecular length scales requires experiments at very low scattering vectors Q. The high interfacial mobility may help in self-repairing non-stabilized interfacial fractions, reducing coalescence.

With these findings we deepen the molecular level understanding of proteins at oil-water interfaces, which can stimulate development of new plant-based emulsion products, and contribute to the global protein transition.

4.1. Statistics

For the statistical analysis Origin (Version 2024b, OriginLab, Northampton, Massachusetts) was used. Differences ($p > 0.05$) were evaluated via one-way ANOVA and a Bonferroni post-hoc test. Data were tested for normality and homogenity using Levene's test before performing ANOVA.

Acknowledgements

A portion of this research used resources at the Spallation Neutron Source, a DOE Office of Science User Facility operated by the Oak Ridge National Laboratory. Beam time at SANS-1 at the SINQ Swiss Spallation Source, PSI, Villigen, was acknowledged. Deuterated MCT oil had been provided by the JCNS deuteration services, Forschungszentrum Jülich.

Author Contributions

T.H.H. was involved in planning the project, conducting SANS experiments, analyzing data, and writing the manuscript. M.M. prepared and characterized samples and participated in SANS experiments. P.S. contributed to the experimental work. O.H. conducted SANS experiments, analyzed data, and contributed to manuscript writing. J.K. also conducted SANS experiments. B.W. carried out the SAXS experiments. H.F. performed data fitting and modeling for both SANS and SAXS, and contributed to manuscript writing. S.F. was responsible for manuscript editing and writing. K.S. synthesized deuterated oil and helped edit the manuscript. J.L., L.S., and Y.J. were involved in writing, reviewing, and editing. P.Z. conducted the NSE experiments.

Conflict of Interest

The authors declare no conflict of interest.

Data Availability Statement

The data that support the findings of this study are available from the corresponding author upon reasonable request.

Keywords

cruciferin, interfaces, motion, scattering, structure

Received: April 25, 2025
Revised: July 18, 2025
Published online:

[1] D. J. McClements, E. Newman, I. F. McClements, *Compr. Rev. Food Sci. Food Saf.* **2019**, *18*, 2047.
[2] D. Plamada, B.-E. Teleky, S. A. Nemes, L. Mitrea, K. Szabo, L.-F. Călinoiu, M. S. Pascuta, R.-A. Varvara, C. Ciont, G. A. Martău, E. Simon, G. Barta, F. V. Dulf, D. C. Vodnar, M. Nitescu, *Foods* **2023**, *12*, 1883.
[3] J. Wanasundara, T. McIntosh, S. Perera, T. Withana-Gamage, P. Mitra, *OCL - Oilseeds fats, Crops, Lipids* **2016**, *23*, 36.
[4] J. Rödin, L. Rask, *Physiol. Plant.* **1990**, *79*, 421.
[5] J. Rödin, L. Rask, *Plant Sci.* **1990**, *70*, 57.
[6] S. P. Perera, T. C. McIntosh, J. P. Wanasundara, *Plants* **2016**, *5*, 36.
[7] J. Yang, P. Shen, A. de Groot, H. Mocking-Bode, C. Nikiforidis, L. Sagis, *J. Colloid Interface Sci.* **2024**, *662*, 192.
[8] P. Shen, J. Yang, C. V. Nikiforidis, H. C. Mocking-Bode, L. M. Sagis, *Food Hydrocolloids* **2023**, *136*, 108300.
[9] A. Akbari, J. Wu, *Food Hydrocolloids* **2016**, *54*, 107.
[10] A. Fetzer, K. Müller, M. Schmid, P. Eisner, *Ind. Crops Prod.* **2020**, *158*, 112986.
[11] T. S. Withana-Gamage, D. D. Hegedus, T. C. McIntosh, C. Coutu, X. Qiu, J. P. Wanasundara, *Food Res. Int.* **2020**, *137*, 109387.
[12] J. Q. Wu, C. D. McCormick, T. D. Pollard, *Methods Cell Biol.* **2008**, *89*, 253.
[13] B. Khaliq, S. Falke, A. Negm, F. Buck, A. Munawar, M. Saqib, S. Mahmood, M. Ahmad, C. Betzel, A. Akrem, *J. Mol. Struct.* **2017**, *1137*, 60.
[14] E. P. Gilbert, *Curr. Opin. Colloid Interface Sci.* **2019**, *42*, 55.
[15] T. Heiden-Hecht, B. Wu, K. Schwärzer, S. Förster, J. Kohlbrecher, O. Holderer, H. Frielinghaus, *J. Colloid Interface Sci.* **2024**, *655*, 319.
[16] A. Lopez-Rubio, E. P. Gilbert, *Trends Food Sci. Technol.* **2009**, *20*, 576.
[17] L. Cheng, A. Ye, Y. Hemar, E. P. Gilbert, L. De Campo, A. E. Whitten, H. Singh, *Langmuir* **2019**, *35*, 12017.
[18] T. Heiden-Hecht, M. Ulbrich, S. Drusch, M. Brueckner-Guehmann, *Food Biophys.* **2021**, *16*, 169.
[19] T. Heiden-Hecht, S. Drusch, *Food Biophys.* **2022**, *17*, 171.
[20] S. Bucciarelli, J. S. Myung, B. Farago, S. Das, G. A. Vliegenthart, O. Holderer, R. G. Winkler, P. Schurtenberger, G. Gompper, A. Stradner, *Sci. Adv.* **2016**, *2*, 1601432.
[21] I. Hoffmann, R. Michel, M. Sharp, O. Holderer, M.-S. Appavou, F. Polzer, B. Farago, M. Gradzielski, *Nanoscale* **2014**, *6*, 6945.
[22] M. G. R. Tandang-Silvas, T. Fukuda, F. Chisato, P. Krisna, C. Cerrone, K. Aiko, I. Takafumi, M. Bunzo, U. Shigeru, M. Nobuyuki, *Biochimica et Biophysica Acta* **2010**, *1804*, 1432.
[23] M. Varadi, D. Bertoni, P. Magana, U. Paramval, I. Pidruchna, M. Radhakrishnan, M. Tsenkov, S. Nair, M. Mirdita, J. Yeo, O. Kovalevskiy, K. Tunyasuvunakool, A. Laydon, A. ž́ídek, H. Tomlinson, D. Hariharan, J. Abrahamson, T. Green, J. Jumper, E. Birney, M. Steinegger, D. Hassabis, S. Velankar, *Nucleic Acids Res.* **2024**, *52*, D368.
[24] L. A. Feigin, D. I. Svergun, et al., *Structure analysis by small-angle X-ray and neutron scattering*, vol. *1*, Springer, New York **1987**, https://doi.org/10.1007/978-1-4757-6624-0.
[25] J. Kohlbrecher, W. Wagner, *J. Appl. Crystallogr.* **2000**, *33*, 804.
[26] U. Keiderling, *Appl. Phys. A* **2002**, *74*, s1455.

[27] (Eds.: F. Mezei, P. C., G. T.), *Neutron Spin Echo Spectroscopy*, Number 601 in Lecture Notes in Physics, Springer, Berlin, Heidelberg, New York, **2003**.
[28] D. Richter, M. Monkenbusch, A. Arbe, J. Colmenero, In *Neutron Spin Echo in Polymer Systems. Advances in Polymer Science*, vol. *174*, Springer, Berlin, Heidelberg, **2005**, pp. 1–221.
[29] M. Ohl, M. Monkenbusch, N. Arend, T. Kozielewski, G. Vehres, C. Tiemann, M. Butzek, H. Soltner, U. Giesen, R. Achten, H. Stelzer, B. Lindenau, A. Budwig, H. Kleines, M. Drochner, P. Kaemmerling, M. Wagener, R. Möller, E. Iverson, M. Sharp, D. Richter, *Nucl. Instrum. Methods Phys. Res., Sect. A* **2013**, *696*, 85.
[30] P. A. Zolnierczuk, O. Holderer, S. Pasini, T. Kozielewski, L. R. Stingaciu, M. Monkenbusch, *J. Appl. Crystallogr.* **2019**, *52*, 1022.
[31] J. Jumper, R. Evans, A. Pritzel, T. Green, M. Figurnov, O. Ronneberger, K. Tunyasuvunakool, R. Bates, A. Žídek, A. Potapenko, A. Bridgland, C. Meyer, S. A. A. Kohl, A. J. Ballard, A. Cowie, B. Romera-Paredes, S. Nikolov, R. Jain, J. Adler, T. Back, S. Petersen, D. Reiman, E. Clancy, M. Zielinski, M. Steinegger, M. Pacholska, T. Berghammer, S. Bodenstein, D. Silver, O. Vinyals, et al., *nature* **2021**, *596*, 583.
[32] M. R. G. Tandang-Silvas, T. Fukuda, C. Fukuda, K. Prak, C. Cabanos, A. Kimura, T. Itoh, B. Mikami, S. Utsumi, N. Maruyama, *Biochim. Biophys. Acta, Proteins Proteomics* **2010**, *1804*, 1432.
[33] D. Svergun, S. Richard, M. Koch, Z. Sayers, S. Kuprin, G. Zaccai, *Proc. Natl. Acad. Sci. USA* **1998**, *95*, 2267.
[34] D. Franke, M. Petoukhov, P. Konarev, A. Panjkovich, A. Tuukkanen, H. Mertens, A. Kikhney, N. Hajizadeh, J. Franklin, C. Jeffries, D. I. Svergun, *J. Appl. Crystallogr.* **2017**, *50*, 1212.
[35] T. Yamaguchi, K. Akao, A. Koutsioubas, H. Frielinghaus, T. Kohzuma, *Biomolecules* **2022**, *12*, 95.
[36] E. Ntone, T. van Wesel, L. M. Sagis, M. Meinders, J. H. Bitter, C. V. Nikiforidis, *J. Colloid Interface Sci.* **2021**, *583*, 459.
[37] K. Schwärzer, T. Heiden-Hecht, Y. Chen, O. Holderer, H. Frielinghaus, P. Li, J. Allgaier, *Eur. J. Org. Chem.* **2023**, *26*, e202300632.
[38] C. Azémard, M.-C. Fauré, S. Stankic, S. Chenot, H. Ibrahim, L. Laporte, P. Fontaine, M. Goldmann, L. de Viguerie, *Langmuir* **2022**, *38*, 711.
[39] D. Cholakova, N. Denkov, *Adv. Colloid Interface Sci.* **2024**, *323*, 103071.
[40] A. Sadeghpour, M. L. Parada, J. Vieira, M. Povey, M. Rappolt, *J. Phys. Chem. B* **2018**, *122*, 10320.
[41] S. Hansen, *J. Appl. Crystallogr.* **2000**, *33*, 1415.
[42] D. Franke, D. I. Svergun, *J. Appl. Crystallogr.* **2009**, *42*, 342.
[43] M. Nagao, *Phys. Rev. E* **2009**, *80*, 031606.
[44] S. Chakraborty, M. Doktorova, T. R. Molugu, F. A. Heberle, H. L. Scott, B. Dzikovski, M. Nagao, L. Stingaciu, R. F. Standaert, F. N. Barrera, J. Katsaras, G. Khelashvili, M. F. Brown, R. Ashkar, *Proc. Nat. Acad. Sci. USA* **2020**, *117*, 21896.
[45] A. G. Zilman, R. Granek, *Phys. Rev. Lett.* **1996**, *77*, 4788.
[46] R. Granek, I. Hoffmann, E. G. Kelley, M. Nagao, P. M. Vlahovska, A. Zilman, *Eur. Phys. J. E* **2024**, *47*, 2.
[47] S. Koizumi, M. Monkenbusch, D. Richter, D. Schwahn, B. Farago, *J. Chem. Phys.* **2004**, *121*, 12721.